ELSEVIER

Physics Letters B 526 (2002) 206–220

PHYSICS LETTERS B

www.elsevier.com/locate/npe

Search for scalar leptons in e^+e^- collisions at centre-of-mass energies up to 209 GeV

ALEPH Collaboration

A. Heister, S. Schael

Physikalisches Institut das RWTH-Aachen, D-52056 Aachen, Germany

R. Barate, R. Brunelière, I. De Bonis, D. Decamp, C. Goy, S. Jezequel, J.-P. Lees, F. Martin, E. Merle, M.-N. Minard, B. Pietrzyk, B. Trocmé

Laboratoire de Physique des Particules (LAPP), IN^2P^3-CNRS, F-74019 Annecy-le-Vieux Cedex, France

G. Boix, S. Bravo, M.P. Casado, M. Chmeissani, J.M. Crespo, E. Fernandez, M. Fernandez-Bosman, Ll. Garrido [15], E. Graugés, J. Lopez, M. Martinez, G. Merino, R. Miquel [31], Ll.M. Mir [31], A. Pacheco, D. Paneque, H. Ruiz

Institut de Física d'Altes Energies, Universitat Autònoma de Barcelona, E-08193 Bellaterra (Barcelona), Spain [7]

A. Colaleo, D. Creanza, N. De Filippis, M. de Palma, G. Iaselli, G. Maggi, M. Maggi, S. Nuzzo, A. Ranieri, G. Raso [24], F. Ruggieri, G. Selvaggi, L. Silvestris, P. Tempesta, A. Tricomi [3], G. Zito

Dipartimento di Fisica, INFN Sezione di Bari, I-70126 Bari, Italy

X. Huang, J. Lin, Q. Ouyang, T. Wang, Y. Xie, R. Xu, S. Xue, J. Zhang, L. Zhang, W. Zhao

Institute of High Energy Physics, Academia Sinica, Beijing, People's Republic of China [8]

D. Abbaneo, P. Azzurri, T. Barklow [30], O. Buchmüller [30], M. Cattaneo, F. Cerutti, B. Clerbaux, H. Drevermann, R.W. Forty, M. Frank, F. Gianotti, T.C. Greening [26], J.B. Hansen, J. Harvey, D.E. Hutchcroft, P. Janot, B. Jost, M. Kado [31], P. Maley,

0370-2693/02/$ – see front matter
PII: S0370-2693(01)01494-0

P. Mato, A. Moutoussi, F. Ranjard, L. Rolandi, D. Schlatter, G. Sguazzoni, W. Tejessy, F. Teubert, A. Valassi, I. Videau, J.J. Ward

European Laboratory for Particle Physics (CERN), CH-1211 Geneva 23, Switzerland

F. Badaud, S. Dessagne, A. Falvard [20], D. Fayolle, P. Gay, J. Jousset, B. Michel, S. Monteil, D. Pallin, J.M. Pascolo, P. Perret

Laboratoire de Physique Corpusculaire, Université Blaise Pascal, IN^{2}P^3-CNRS, Clermont-Ferrand, F-63177 Aubière, France

J.D. Hansen, J.R. Hansen, P.H. Hansen, B.S. Nilsson, A. Wäänänen

Niels Bohr Institute, 2100 Copenhagen, DK-Denmark [9]

A. Kyriakis, C. Markou, E. Simopoulou, A. Vayaki, K. Zachariadou

Nuclear Research Center Demokritos (NRCD), GR-15310 Attiki, Greece

A. Blondel [12], J.-C. Brient, F. Machefert, A. Rougé, M. Swynghedauw, R. Tanaka, H. Videau

Laboratoire de Physique Nucléaire et des Hautes Energies, Ecole Polytechnique, IN^{2}P^3-CNRS, F-91128 Palaiseau Cedex, France

V. Ciulli, E. Focardi, G. Parrini

Dipartimento di Fisica, Università di Firenze, INFN Sezione di Firenze, I-50125 Firenze, Italy

A. Antonelli, M. Antonelli, G. Bencivenni, G. Bologna [4], F. Bossi, P. Campana, G. Capon, V. Chiarella, P. Laurelli, G. Mannocchi [5], F. Murtas, G.P. Murtas, L. Passalacqua, M. Pepe-Altarelli [25], P. Spagnolo

Laboratori Nazionali dell'INFN (LNF-INFN), I-00044 Frascati, Italy

J. Kennedy, J.G. Lynch, P. Negus, V. O'Shea, D. Smith, A.S. Thompson

Department of Physics and Astronomy, University of Glasgow, Glasgow G12 8QQ, United Kingdom [10]

S. Wasserbaech

Department of Physics, Haverford College, Haverford, PA 19041-1392, USA

R. Cavanaugh, S. Dhamotharan, C. Geweniger, P. Hanke, V. Hepp, E.E. Kluge, G. Leibenguth, A. Putzer, K. Tittel, S. Werner [19], M. Wunsch [19]

Kirchhoff-Institut für Physik, Universität Heidelberg, D-69120 Heidelberg, Germany [16]

R. Beuselinck, D.M. Binnie, W. Cameron, G. Davies, P.J. Dornan, M. Girone [1], R.D. Hill, N. Marinelli, J. Nowell, H. Przysiezniak [2], S.A. Rutherford, J.K. Sedgbeer, J.C. Thompson [14], R. White

Department of Physics, Imperial College, London SW7 2BZ, United Kingdom [10]

V.M. Ghete, P. Girtler, E. Kneringer, D. Kuhn, G. Rudolph

Institut für Experimentalphysik, Universität Innsbruck, A-6020 Innsbruck, Austria [18]

E. Bouhova-Thacker, C.K. Bowdery, D.P. Clarke, G. Ellis, A.J. Finch, F. Foster, G. Hughes, R.W.L. Jones, M.R. Pearson, N.A. Robertson, M. Smizanska

Department of Physics, University of Lancaster, Lancaster LA1 4YB, United Kingdom [10]

V. Lemaitre

Institut de Physique Nucléaire, Département de Physique, Université Catholique de Louvain, 1348 Louvain-la-Neuve, Belgium

U. Blumenschein, F. Hölldorfer, K. Jakobs, F. Kayser, K. Kleinknecht, A.-S. Müller, G. Quast [6], B. Renk, H.-G. Sander, S. Schmeling, H. Wachsmuth, C. Zeitnitz, T. Ziegler

Institut für Physik, Universität Mainz, D-55099 Mainz, Germany [16]

A. Bonissent, J. Carr, P. Coyle, C. Curtil, A. Ealet, D. Fouchez, O. Leroy, T. Kachelhoffer, P. Payre, D. Rousseau, A. Tilquin,

Centre de Physique des Particules de Marseille, Univ. Méditerranée, IN^{2}P^3-CNRS, F-13288 Marseille, France

F. Ragusa

Dipartimento di Fisica, Università di Milano e INFN Sezione di Milano, I-20133 Milano, Italy

A. David, H. Dietl, G. Ganis [27], K. Hüttmann, G. Lütjens, C. Mannert, W. Männer, H.-G. Moser, R. Settles, H. Stenzel, G. Wolf

Max-Planck-Institut für Physik, Werner-Heisenberg-Institut, D-80805 München, Germany [16]

J. Boucrot, O. Callot, M. Davier, L. Duflot, J.-F. Grivaz, Ph. Heusse, A. Jacholkowska [20], C. Loomis, L. Serin, J.-J. Veillet, J.-B. de Vivie de Régie [28], C. Yuan

Laboratoire de l'Accélérateur Linéaire, Université de Paris-Sud, IN^{2}P^3-CNRS, F-91898 Orsay Cedex, France

G. Bagliesi, T. Boccali, L. Foà, A. Giammanco, A. Giassi, F. Ligabue, A. Messineo, F. Palla, G. Sanguinetti, A. Sciabà, R. Tenchini [1], A. Venturi [1], P.G. Verdini

Dipartimento di Fisica dell'Università, INFN Sezione di Pisa, e Scuola Normale Superiore, I-56010 Pisa, Italy

O. Awunor, G.A. Blair, J. Coles, G. Cowan, A. Garcia-Bellido, M.G. Green, L.T. Jones, T. Medcalf, A. Misiejuk, J.A. Strong, P. Teixeira-Dias

Department of Physics, Royal Holloway & Bedford New College, University of London, Egham, Surrey TW20 OEX, United Kingdom [10]

R.W. Clifft, T.R. Edgecock, P.R. Norton, I.R. Tomalin

Particle Physics Department, Rutherford Appleton Laboratory, Chilton, Didcot, Oxon OX11 OQX, United Kingdom [10]

B. Bloch-Devaux [1], D. Boumediene, P. Colas, B. Fabbro, E. Lançon, M.-C. Lemaire, E. Locci, P. Perez, J. Rander, J.-F. Renardy, A. Rosowsky, P. Seager [13], A. Trabelsi [21], B. Tuchming, B. Vallage

CEA, DAPNIA/Service de Physique des Particules, CE-Saclay, F-91191 Gif-sur-Yvette Cedex, France [17]

N. Konstantinidis, A.M. Litke, G. Taylor

Institute for Particle Physics, University of California at Santa Cruz, Santa Cruz, CA 95064, USA [22]

C.N. Booth, S. Cartwright, F. Combley [4], P.N. Hodgson, M. Lehto, L.F. Thompson

Department of Physics, University of Sheffield, Sheffield S3 7RH, United Kingdom [10]

K. Affholderbach [23], A. Böhrer, S. Brandt, C. Grupen, J. Hess, A. Ngac, G. Prange, U. Sieler

Fachbereich Physik, Universität Siegen, D-57068 Siegen, Germany [16]

C. Borean, G. Giannini

Dipartimento di Fisica, Università di Trieste e INFN Sezione di Trieste, I-34127 Trieste, Italy

H. He, J. Putz, J. Rothberg

Experimental Elementary Particle Physics, University of Washington, Seattle, WA 98195, USA

S.R. Armstrong, K. Berkelman, K. Cranmer, D.P.S. Ferguson, Y. Gao [29], S. González, O.J. Hayes, H. Hu, S. Jin, J. Kile, P.A. McNamara III, J. Nielsen, Y.B. Pan,

J.H. von Wimmersperg-Toeller, W. Wiedenmann, J. Wu, S.L. Wu, X. Wu, G. Zobernig

Department of Physics, University of Wisconsin, Madison, WI 53706, USA [11]

G. Dissertori

Institute for Particle Physics, ETH Hönggerberg, HPK, 8093 Zürich, Switzerland

Received 4 December 2001; received in revised form 18 December 2001; accepted 20 December 2001

Editor: L. Montanet

Abstract

A search for selectron, smuon and stau pair production is performed with the data collected by the ALEPH detector at LEP at centre-of-mass energies up to 209 GeV. The numbers of candidate events are consistent with the background predicted by the Standard Model. Final mass limits from ALEPH are reported.

[1] Also at CERN, 1211 Geneva 23, Switzerland.
[2] Now at LAPP, 74019 Annecy-le-Vieux, France.
[3] Also at Dipartimento di Fisica di Catania and INFN Sezione di Catania, 95129 Catania, Italy.
[4] Deceased.
[5] Also Istituto di Cosmo-Geofisica del C.N.R., Torino, Italy.
[6] Now at Institut für Experimentelle Kernphysik, Universität Karlsruhe, 76128 Karlsruhe, Germany.
[7] Supported by CICYT, Spain.
[8] Supported by the National Science Foundation of China.
[9] Supported by the Danish Natural Science Research Council.
[10] Supported by the UK Particle Physics and Astronomy Research Council.
[11] Supported by the US Department of Energy, grant DE-FG0295-ER40896.
[12] Now at Departement de Physique Corpusculaire, Université de Genève, 1211 Genève 4, Switzerland.
[13] Supported by the Commission of the European Communities, contract ERBFMBICT982874.
[14] Also at Rutherford Appleton Laboratory, Chilton, Didcot, UK.
[15] Permanent address: Universitat de Barcelona, 08208 Barcelona, Spain.
[16] Supported by the Bundesministerium für Bildung, Wissenschaft, Forschung und Technologie, Germany.
[17] Supported by the Direction des Sciences de la Matière, C.E.A.
[18] Supported by the Austrian Ministry for Science and Transport.
[19] Now at SAP AG, 69185 Walldorf, Germany.
[20] Now at Groupe d'Astroparticules de Montpellier, Université de Montpellier II, 34095 Montpellier, France.
[21] Now at Département de Physique, Faculté des Sciences de Tunis, 1060 Le Belvédère, Tunisia.
[22] Supported by the US Department of Energy, grant DE-FG03-92ER40689.
[23] Now at Skyguide, Swissair Navigation Services, Geneva, Switzerland.
[24] Also at Dipartimento di Fisica e Tecnologie Relative, Università di Palermo, Palermo, Italy.
[25] Now at CERN, 1211 Geneva 23, Switzerland.
[26] Now at Honeywell, Phoenix AZ, USA.
[27] Now at INFN Sezione di Roma II, Dipartimento di Fisica, Università di Roma Tor Vergata, 00133 Roma, Italy.
[28] Now at Centre de Physique des Particules de Marseille, Univ. Méditerranée, F-13288 Marseille, France.
[29] Also at Department of Physics, Tsinghua University, Beijing, People's Republic of China.
[30] Now at SLAC, Stanford, CA 94309, USA.
[31] Now at LBNL, Berkeley, CA 94720, USA.

1. Introduction

The final results of searches for sleptons ($\tilde{\ell}$) with the data collected by the ALEPH detector at LEP at centre-of-mass energies up to 209 GeV are presented in this Letter. These searches are interpreted in the theoretical framework of the minimal supersymmetric extension of the Standard Model (MSSM) [1], with R-parity conservation and the assumption that the lightest neutralino is the lightest supersymmetric particle (LSP).

Scalar leptons are pair produced at LEP through s-channel exchange of a Z or a γ giving rise to either $\tilde{\ell}_L\tilde{\ell}_L$ or $\tilde{\ell}_R\tilde{\ell}_R$. Selectrons can also be produced through the t-channel exchange of a neutralino, resulting also in $\tilde{\mathrm{e}}_L\tilde{\mathrm{e}}_R$ production. Since the amount of mixing between the two slepton states ($\tilde{\ell}_L$ and $\tilde{\ell}_R$) is proportional to the ratio of the lepton mass to the slepton mass, it is negligible for selectrons and smuons and may be sizeable for staus. As a consequence, the stau production cross section depends on the MSSM parameters A_τ, μ and $\tan\beta$ via stau mixing, while the smuon production cross section depends only on the smuon mass. A dependence on M_1, M_2, μ and $\tan\beta$ is also present for the selectron cross section via the couplings with the neutralino in the t-channel production.

In most of the MSSM parameter space, sleptons decay predominantly into their Standard Model (SM) partners and the lightest neutralino, $\tilde{\ell}^{\pm} \to \ell^{\pm}\chi_1^0$. The experimental signature is therefore a pair of oppositely-charged, same-flavour, acoplanar leptons (electrons, muons or taus), accompanied with missing energy carried away by the two undetected neutralinos.

Results of previous slepton searches up to $\sqrt{s} = 202$ GeV have been reported by ALEPH [2–4] and by the other LEP Collaborations [5]. In this Letter the analyses performed on the data taken in the year 2000 at centre-of-mass energies ranging from 204 to 209 GeV are presented. The selections are mostly independent of the centre-of-mass energy except for an appropriate rescaling of the cuts with $\sqrt{s}$ when relevant. The results are combined with those obtained with previous data collected from 1997 to 1999. The luminosities and centre-of-mass energies are shown in Table 1.

This Letter is organised as follows. In Section 2, a brief description of the ALEPH detector is given.

Table 1
Integrated luminosities, centre-of-mass energy ranges and mean centre-of-mass energy values for data collected by the ALEPH detector from 1997 to 2000

Year	Luminosity (pb^{-1})	Energy range (GeV)	$\langle\sqrt{s}\rangle$ (GeV)
2000	9.4	207–209	208.0
	122.6	206–207	206.6
	75.3	204–206	205.2
1999	42.0	–	201.6
	86.2	–	199.5
	79.8	–	195.5
	28.9	–	191.6
1998	173.6	–	188.6
1997	56.8	–	182.7

The signal and background simulations are presented in Section 3. In Section 4, the selection criteria are described. Systematic uncertainties are discussed in Section 5. The results are reported in Section 6.

2. ALEPH detector

The ALEPH detector is described in detail in Ref. [6]. An account of its performance and a description of the standard analysis algorithms can be found in Ref. [7].

In ALEPH, the trajectories of charged particles are measured with a silicon vertex detector, a cylindrical drift chamber, and a large time projection chamber (TPC). These detector components are immersed in a 1.5 T axial magnetic field provided by a superconducting solenoidal coil. Reconstructed charged particle trajectories are called *good tracks* if they are reconstructed with at least four space points in the TPC, a transverse momentum in excess of 200 MeV/c, a polar angle with respect to the beam such that $|\cos\theta| < 0.95$, and originating from within a cylinder of length 10 cm and radius 2 cm coaxial with the beam and centred at the nominal interaction point.

The electromagnetic calorimeter (ECAL), placed between the TPC and the coil, is a highly-segmented, 22-radiation-length-thick sandwich of lead planes and proportional wire chambers. It consists of a barrel and two endcaps. It is used to identify electrons and photons by the characteristic longitudinal and transverse developments of the associated showers, sup-

plemented for low momentum electrons by the measurement in the TPC of the specific energy loss by ionization. Photon conversions to e^+e^- are identified as pairs of oppositely-charged electrons satisfying stringent conditions on their distance of closest approach and their invariant mass. The luminosity monitors (LCAL and SiCAL) extend the ECAL hermeticity down to 34 mrad from the beam axis. The hadron calorimeter (HCAL) consists of the iron return yoke of the magnet instrumented with streamer tubes. It provides a measurement of the hadronic energy and, together with the external muon chambers, efficient identification of muons by their characteristic penetration pattern.

Global event quantities (such as total energy and missing momentum) are determined with an energy-flow algorithm which combines all the above measurements into charged particles (electrons, muons and charged hadrons), photons and neutral hadrons, called *energy-flow particles* in the following. Tau identification proceeds by clustering the energy-flow particles into two jets with the Durham algorithm [8]. A jet is called a tau-jet candidate if it contains one or three good track(s) (or two if it contains an identified electron, to allow for asymmetric photon conversions) and if the jet invariant mass is smaller than 2 GeV/c^2.

3. Simulated samples

The signal samples were generated using SUSYGEN [9], with final state radiation simulated with the PHOTOS [10] package and tau decays simulated with TAUOLA [11]. The slepton masses were varied in steps of 5 GeV/c^2 (1 GeV/c^2) for a mass difference ΔM with the lightest neutralino larger (smaller) than 10 GeV/c^2; the mass of the neutralino was varied in steps of 5 GeV/c^2.

Event samples of all SM background processes relevant for the slepton search were also generated, i.e., dilepton production, $\gamma\gamma$ interactions with leptonic final states, W and Z pair production, and Zee and Weν production. The Bhabha process was simulated with BHWIDE [12], muon and tau pair production with KORALZ [13], the $\gamma\gamma$ processes with PHOT02 [14], WW production with KORALW [15] and the remaining four-fermion processes with PYTHIA [16].

A detailed GEANT [17] simulation of the detector response was applied to both background and signal events.

4. Description of the selections

The final state topology depends on the slepton flavour. Selectrons and smuons are selected by requiring exactly two good tracks identified as electrons or muons and with opposite electric charge, while staus are selected by requiring two to six good tracks, clustered into two tau-jet candidates. The final state topology also depends on ΔM. Because the backgrounds are different for large values of ΔM (mostly W pair production) and small values of ΔM (mostly $\gamma\gamma$ interactions), the selections were optimized for two ΔM ranges. They are called "small-ΔM" and "large-ΔM" analyses in the following. The selections were optimized by minimizing the signal cross section expected to be excluded, on average, in absence of signal (the $\overline{N}_{95}$ prescription [18]). The selection criteria are summarized in Table 2 for selectrons and smuons and in Table 3 for staus. The variables used in both the small- and large-ΔM analyses are defined below.

- Acoplanarity Φ_{aco}

The acoplanarity is defined as the angle between the two lepton momenta projected onto the plane transverse to the beam. An acoplanarity cut is used to reject events from $e^+e^- \to \ell^+\ell^-$ or $\gamma\gamma \to \ell^+\ell^-$.

- The ρ variable

The lepton momenta are projected onto the transverse plane and the thrust axis is computed from the projected momenta. The ρ variable is defined as the scalar sum of the transverse momentum components of all energy-flow particles with respect to the thrust axis. A cut on ρ reduces the number of background events from the $e^+e^- \to \tau^+\tau^-$ and $\gamma\gamma \to \tau^+\tau^-$ processes.

- Variables M_{vis}, p_{miss}, θ_{miss}, ϕ_{miss}, p_{Tmiss} and p_{Lmiss}

The total energy and momentum is constructed by adding energies and momenta of all energy-flow particles of the event, allowing a total visible mass M_{vis} to be computed. The missing momentum p_{miss}, identical in magnitude and opposite in direction to the total momentum, defines the variables θ_{miss} and ϕ_{miss} (polar and azimuthal angles of its direction), and

Table 2
Selection criteria for the searches for acoplanar selectrons and smuons. The energies are expressed in GeV, the momenta in GeV/c and the masses in GeV/c^2. Di-fermion final state events, four-fermion final state events and photon conversions are denoted by 2f, 4f and γ conv., respectively. The sliding energy cut is explained in Section 6

		Selectron and smuon selection criteria	
		Large ΔM ($\Delta M > 12$)	Small ΔM ($\Delta M < 12$)
Preselection	Good tracks	Two oppositely-charged, same-flavour, identified e or μ	
Anti-2f	Acoplanarity	$\Phi_{\rm aco} < 170^\circ$	
Anti-(2f + γ)	Neutral veto	Cut applied	
Anti-(γ conv.)	Acollinearity	$\alpha > 2^\circ$	
Anti-$\gamma\gamma$	Energy within 12°	$E_{12} = 0$ (Threshold: 90 MeV)	$E_{12}(\mathrm{H}) = 0$ (Threshold: 90 MeV)
	Visible mass	$M_{\rm vis} > 4$	$M_{\rm vis}(\mathrm{nH}) > 4$
	ρ	$\rho > 2$	$\rho > 1$
	Missing momentum	$p_{\rm Tmiss} > 3\%\sqrt{s}$	$p_{\rm Tmiss}(\mathrm{nH}) > 1\%\sqrt{s}$
		if $\lvert\cos\phi_{\rm miss}\rvert < 0.26$,	$p_{\rm Tmiss}(\mathrm{tr}) > 1\%\sqrt{s}$
		then $p_{\rm Tmiss} > 5\%\sqrt{s}$	$\lvert\cos\theta_{\rm miss}(\mathrm{nH})\rvert < 0.9$
	Fisher variable	–	Cut applied
Anti-4f	Lept. momenta	$p_{\rm T1}, p_{\rm T2} > 0.5\%\sqrt{s}$	
		$p_1 < 46.5\%\sqrt{s}$	$p_{\rm T1} < 10\%\sqrt{s}$
	Visible mass	–	$M_{\rm vis}(\mathrm{nH}) < 20\%\sqrt{s}$
	Miss. momentum	–	$p_{\rm miss}(\mathrm{nH}) < 10\%\sqrt{s}$
		Sliding energy cut	

$p_{\rm Tmiss}$ and $p_{\rm Lmiss}$ (transverse and longitudinal components). Because the small-ΔM analysis is more sensitive to accidental double counting between low energy tracks and calorimeter clusters, two alternative methods are used to determine the total energy and momentum, (i) without the neutral hadrons (variables labelled "nH"); and (ii) without the neutral particles (variables labelled "tr"). The cuts on the visible mass and on the missing momentum (value and angle) reject background events from $\gamma\gamma$ processes. The cut on $p_{\rm Tmiss}$ is tightened when the missing momentum points to the vertical boundaries between the two halves of the LCAL.

- Lepton momenta p_1, p_2 and $p_{\rm T1}$

The variable p_1 (p_2) is the momentum of the more (less) energetic identified electron or muon, if any. For massive neutralinos, upper cuts on $M_{\rm vis}$ and p_1 are effective at rejecting leptonic WW events.

- Activity at small angle E_{12} and $E_{12}(\mathrm{H})$

Because $\gamma\gamma$ interactions often produce particles strongly boosted forward or backward, the requirement that no energy be detected at low angles is effective in suppressing this background. The variable E_{12} gives the total energy measured within 12° of the beam axis in LCAL and SiCAL, and in the first cells (closest to the beam pipe) of the ECAL endcap calorimeters. The variable $E_{12}(\mathrm{H})$ takes into account in addition the energy collected in the first cells of the HCAL endcap calorimeters. This cut introduces an inefficiency due to beam related background (Section 5).

- Neutral veto

Dilepton events with hard initial or final state radiation at large angle from incoming and outgoing leptons give rise to acoplanar lepton pairs, and to potentially large missing energy if the radiated pho-

Table 3
Selection criteria for the search for acoplanar staus. The energies are expressed in GeV, the momenta in GeV/c and the masses in GeV/c^2. Di-fermion final state events, four-fermion final state events and photon conversions are denoted by 2f, 4f and γ conv., respectively. The p_τ variable represents the smaller tau-jet momentum. The sliding energy cut is explained in Section 6

		Stau selection criteria	
		Large ΔM ($\Delta M > 30$)	Small ΔM ($\Delta M < 30$)
Preselection	Good tracks	Two to six tracks clustered in two τ jet candidates	
		$p_\tau \times 206/\sqrt{s} > 1.07$	–
Anti-(γ conv.)	Acollinearity	$\alpha > 2^\circ$	
Anti-(2f + γ)	Neutral veto	yes	
Anti-2f	Acoplanarity and ρ	$\rho \times 206/\sqrt{s} > (\Phi_{\rm aco} - 150^\circ)/7.34$	
Anti-$\gamma\gamma$	Energy within 12°	$E_{12} = 0$ (Threshold: 90 MeV)	
	Visible mass	$M_{\rm vis} > 4$	
	Missing momentum	$p_{\rm Tmiss} \times 206/\sqrt{s} > 16.4 - M_{\rm vis} \times 0.27$	$p_{\rm Tmiss} \times 206/\sqrt{s} > 20.6 - 4.5 \times \rho \times 206/\sqrt{s}$
		$p_{\rm Tmiss} \times 206/\sqrt{s} < (\theta_{\rm miss} - 10^\circ) \times 1.24$	
Anti-4f	Lept. momenta	$p_1 \times 206/\sqrt{s} < 20.0$	$p_1 \times 206/\sqrt{s} < 12.6$
	Visible mass	$M_{\rm vis} < 80.0$	–
		Sliding energy cut	

tons go into poorly instrumented regions of the detector (e.g., ECAL module boundaries, overlap between barrel and endcaps). To reject these events, it is required that the invariant mass between any good track and any neutral energy-flow particle, outside a cone of half-angle 10° around the good track and with an energy in excess of 4 GeV, be smaller than 2 GeV/c^2.

- Acollinearity α

Single-photon events from $e^+e^- \to \nu\bar{\nu}\gamma$ with a hard radiated photon, followed by a photon conversion into an e^+e^- pair, are not rejected by the previous veto, but are characterized by a very small opening angle between the two tracks (called the acollinearity angle). An acollinearity cut is therefore effective at rejecting these events.

- Fisher variable

In order to further reduce the large $\gamma\gamma$ background in the case of the small-ΔM selectron or smuon analyses, a Fisher discriminant [19] analysis is used. This method exploits the remaining modest difference among $\gamma\gamma$ events and the signal, taking into account the correlations between the variables $M_{\rm vis}$, $p_{\rm Tmiss}$, $p_{\rm Lmiss}$, ρ, p_1, p_2, and α.

5. Systematic effects

The main systematic uncertainties on the background and signal expectations come from the statistics of the simulated samples (from 1.5 to 3.5%). A 2% systematic uncertainty was estimated for the lepton identification efficiency. The inefficiency caused by the E_{12} cuts is determined from events triggered at random beam crossings. The corrections for E_{12} (E_{12}(H)) used for the year 2000 data are −9.5% (−14.6%) at 205.2 GeV and −8.8% (−13.7%) at 206.6 and 208.0 GeV. The uncertainties on these corrections are less than 1%.

The numbers of background events and the selection efficiencies are interpolated from the generated values to the mean energies of the year 2000 data. The contribution to the systematic uncertainty of this interpolation procedure is negligible. A comparison between data and expected backgrounds from SM processes is presented in Fig. 1 for the large-ΔM analysis before anti-four-fermion cuts and without lepton identification. At this level, agreement is observed between data and the expected backgrounds, dominated by W pair production.

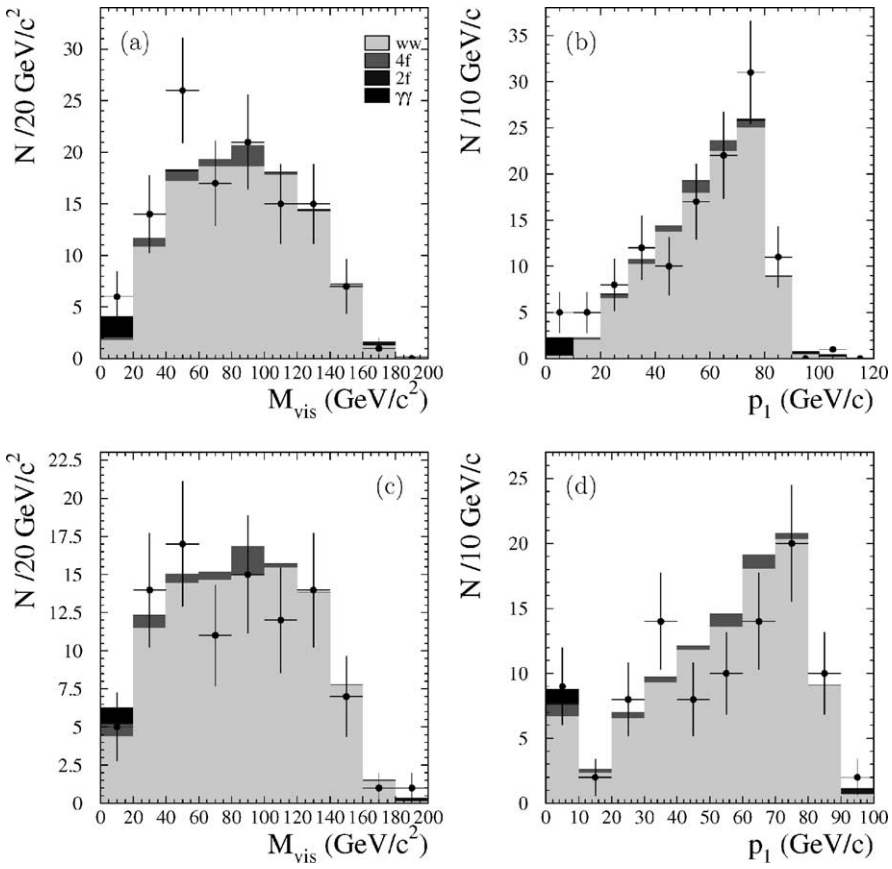

Fig. 1. Comparison between data (dots with error bars) and expected backgrounds (histograms) before anti-four-fermion and lepton identification cuts. For selectrons and smuons: (a) total visible mass (M_{vis}) and (b) momentum of the leading lepton (p_1). For staus: (c) total visible mass (M_{vis}) and (d) momentum of the leading lepton identified in the tau jet (p_1). The accumulation at zero in (d) corresponds to events with no leptons in either tau jet.

6. Results

After the selection criteria described in Section 4 are applied, the numbers of candidate events observed in the data and those expected from SM background processes are given in Table 4 for the selectron and smuon searches and in Table 5 for the stau search.

The search for sleptons is performed as a function of the hypothetical slepton and neutralino masses. A sliding energy cut is applied (not accounted for in Tables 4 and 5) which requires that the lepton momenta be in the range kinematically allowed for a signal with the assumed values of slepton and neutralino masses. For a two-body decay $\tilde{\ell}^{\pm} \to \ell^{\pm}\chi_1^0$, the minimum and maximum values for the decay lepton energy are given by

$$E_{\ell}^{\mathrm{max,min}} = \frac{E_{\mathrm{b}}}{2}\left(1 - \frac{m_{\chi_1^0}^2}{m_{\tilde{\ell}}^2}\right)\left[1 \pm \sqrt{1 - \frac{m_{\tilde{\ell}}^2}{E_{\mathrm{b}}^2}}\right], \quad (1)$$

where E_{b} is the beam energy and where the lepton mass is neglected. In the case of staus, the exact formula is used to account for the non-negligible mass of the tau. An event is compatible with the mass hypothesis $(m_{\tilde{\ell}}, m_{\chi_1^0})$ if both decay leptons satisfy Eq. (1). Any given event may therefore be compatible with a wide mass range, especially for large-ΔM values. In the decay of a stau, the resulting tau lepton will itself give rise to at least one neutrino and the lower limit on the energy cannot be applied. Only the

Table 4
Numbers of candidate events observed in the year 2000 data (N_{obs}) and of background events expected from SM processes (N_{bkg}), in the searches for selectrons and smuons (before the sliding energy cut). The numbers in parentheses give the WW contribution

$\sqrt{s}$ (GeV)	$\tilde{e}$				$\tilde{\mu}$			
	Small ΔM		Large ΔM		Small ΔM		Large ΔM	
	N_{obs}	N_{bkg}	N_{obs}	N_{bkg}	N_{obs}	N_{bkg}	N_{obs}	N_{bkg}
205.2	0	0.12 (0.09)	15	14.0 (12.2)	0	0.12 (0.07)	8	12.5 (11.4)
206.6	0	0.19 (0.16)	24	22.9 (20.0)	0	0.20 (0.11)	28	20.6 (18.8)
208.0	0	0.02 (0.01)	0	1.76 (1.53)	0	0.17 (0.08)	3	1.59 (1.44)

Table 5
Numbers of candidate events observed in the year 2000 data (N_{obs}) and of background events expected from SM processes (N_{bkg}), in the search for staus (before the sliding energy cut). The numbers in parentheses give the WW contribution

$\sqrt{s}$ (GeV)	$\tilde{\tau}$					
	Small ΔM		Large ΔM		Small or large ΔM	
	N_{obs}	N_{bkg}	N_{obs}	N_{bkg}	N_{obs}	N_{bkg}
205.2	5	6.1 (5.0)	1	5.4 (4.4)	5	7.6 (6.3)
206.6	12	10.1 (8.3)	10	8.8 (7.2)	15	12.5 (10.3)
208.0	3	0.80 (0.68)	0	0.70 (0.57)	3	1.01 (0.83)

Table 6
Efficiencies of the selection criteria for different values of the slepton and neutralino masses, at $\sqrt{s} = 208$ GeV

	$m_{\tilde{\ell}}$ (GeV/c^2)	$m_{\chi_1^0}$ (GeV/c^2)	ϵ (%)
$\tilde{e}$	95	0	59
	95	80	54
	95	90	15
$\tilde{\mu}$	90	0	61
	90	75	58
	90	85	20
$\tilde{\tau}$	80	30	30
	80	70	21
	80	75	3

upper limit can be used, which increases even further the compatible region. For the selectron, smuon and stau searches, the numbers of candidate events and expected background events are displayed in Fig. 2 as a function of the slepton and the neutralino masses, after the sliding energy cut is applied. For illustration, the selection efficiencies are given in Table 6 for different values of the slepton and neutralino masses, and at $\sqrt{s} = 208$ GeV.

6.1. Cross section upper limits

The data show no evidence for an excess of events compared to the estimated background. The dominant WW background theoretically and experimentally well under control, is subtracted to derive 95% C.L. upper limits on the slepton production cross section times the branching ratio into $\ell\chi_1^0\ell\chi_1^0$. This partial background subtraction is performed with the likelihood ratio method [20]. Data from previous years are combined in the likelihood to increase the sensitivity. The systematic uncertainties on the efficiencies are taken into account with the method of Ref. [21].

The resulting bounds on the number of signal events produced in the whole data sample are expressed in term of bounds on the production cross section computed at $\sqrt{s} = 208$ GeV, shown in Fig. 3. Cross sections exceeding 0.1 (0.2) pb are excluded in a significant part of the plane $(m_{\tilde{\ell}}, m_{\chi_1^0})$ for selectrons and smuons (staus). In the small-ΔM region, the limits are less stringent because the softer decay leptons cause a drop in the selection efficiency. The limits are also less stringent for slepton masses close to the kinematic limit, where only part of the data contributes.

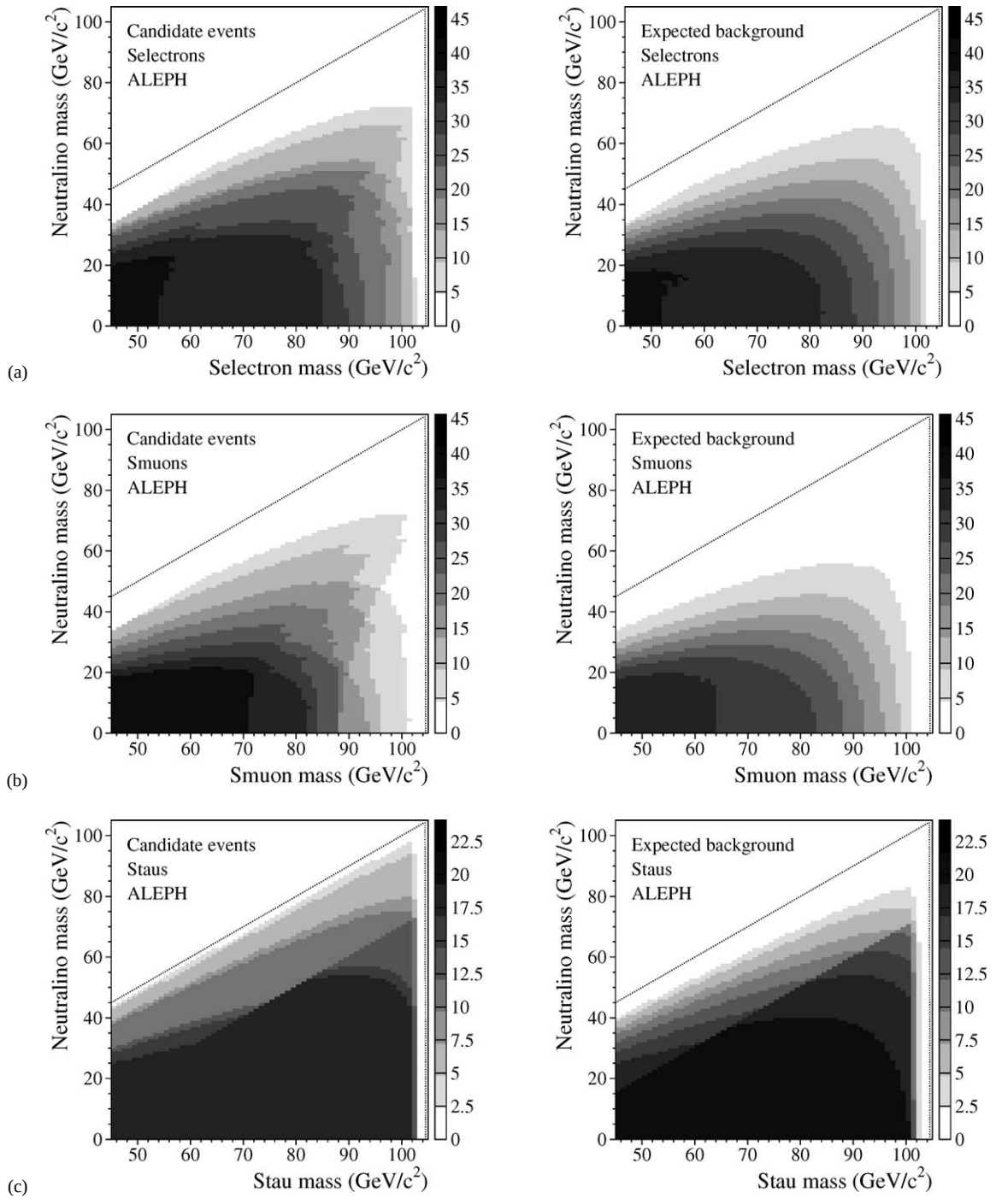

Fig. 2. Numbers of selected events in the year 2000 data (left) and of expected background events from SM processes (right) in the search for (a) selectrons, (b) smuons and (c) staus. The density of shading reflects the number of events as indicated by the vertical scales. The kinematically accessible region at 209 GeV is indicated by the vertical dotted lines. The diagonal dotted lines show the boundary of the domain allowed in the MSSM for a neutralino LSP.

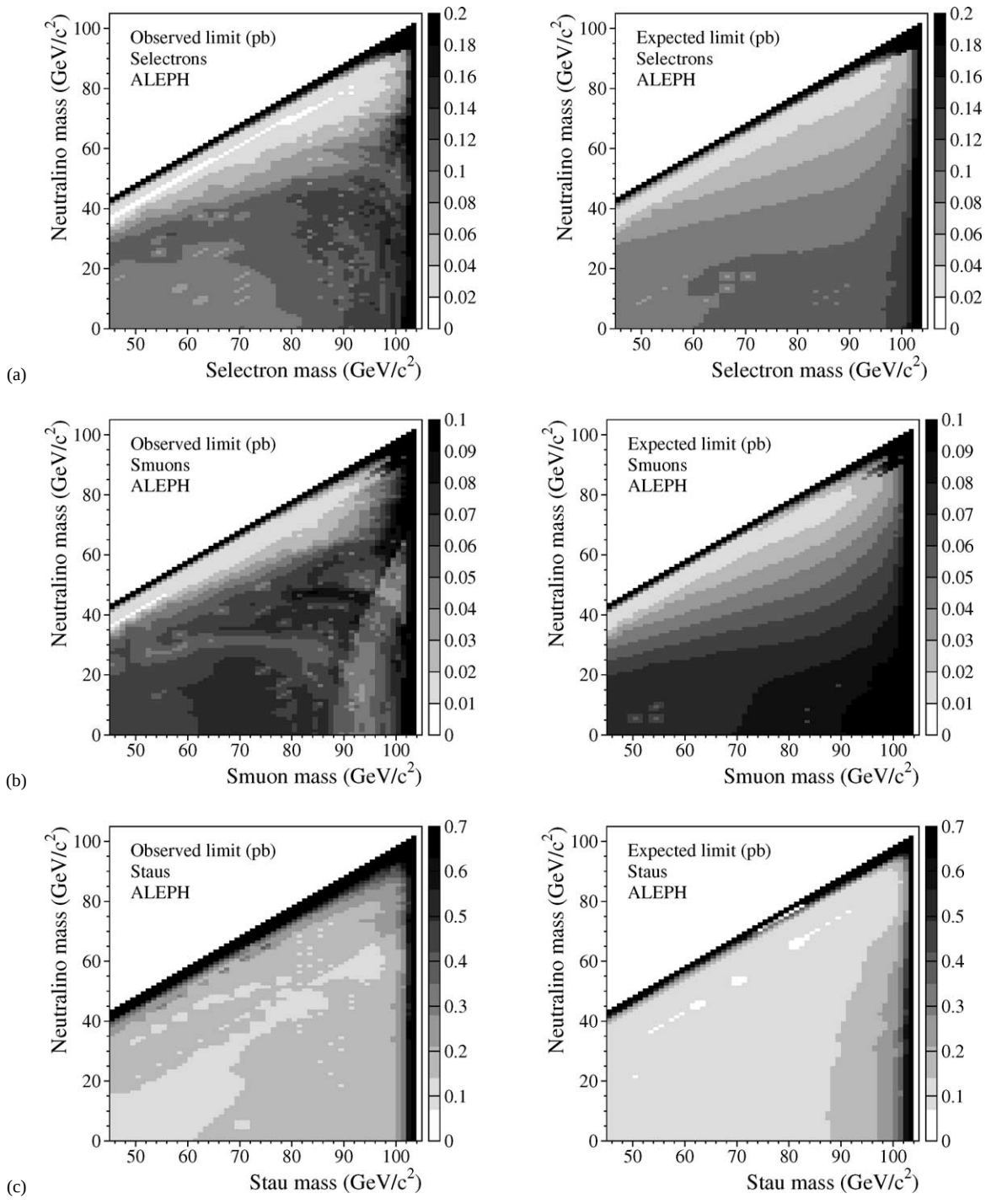

Fig. 3. Upper limit at 95% C.L. on the observed (left) and expected (right) production cross section at $\sqrt{s} = 208$ GeV, times the branching ratio into $\ell\chi_1^0\ell\chi_1^0$ for (a) selectrons, (b) smuons and (c) staus.

6.2. Mass exclusion limits

In the MSSM framework, the previous bounds allow limits to be set on the slepton masses as a function of the neutralino mass. To this end, cross sections and branching ratios are calculated with the program SUSYGEN [9]. For selectrons and smuons, mixing is expected to be negligible and limits are derived under the conservative assumption that only $\tilde{\ell}_R\tilde{\ell}_R$ production contributes. Limits are determined for staus in mixed and unmixed scenarios. Without mixing, conservative limits are set again under the assumption that only $\tilde{\tau}_R\tilde{\tau}_R$ production contributes. If the no-mixing assumption is relaxed, the most conservative limit on the mass of the lightest stau $\tilde{\tau}_1$ is obtained with a mixing angle $\theta_{\tilde{\tau}}$ which minimizes the production cross section ($\theta_{\tilde{\tau}} \simeq 52°$).

The unification of gaugino masses at the GUT scale is assumed for the computations of the slepton branching ratios and of the selectron production cross section. Branching ratios for the slepton decay are calculated for $\mu = -200$ GeV/c^2 and $\tan\beta = 2$. The branching ratio into $\ell^{\pm}\chi_1^0$ is nearly 100% except for small neutralino masses, in which case the cascade decay into $\ell^{\pm}\chi_2^0$ followed by $\chi_2^0 \to \chi_1^0 f\bar{f}$ or $\chi_1^0\gamma$ may become kinematically allowed. The limits are computed under the conservative assumption that the selection efficiency for decay channels other than $\tilde{\ell}^{\pm} \to \ell^{\pm}\chi_1^0$ is zero.

The 95% C.L. expected and observed bounds on the masses of selectrons, smuons and staus as a function of the neutralino mass are displayed in Fig. 4, together with the effect of cascade decays. For staus, the limit obtained with mixing angle $\theta_{\tilde{\tau}} \simeq 52°$ is also given. The observed stau mass limit is less stringent than expected because a small excess of events was observed in 1999 [4].

The 95% C.L. bounds on the slepton masses for $\Delta M > 15$ GeV/c^2 are summarized in Table 7, with the hypothesis BR($\tilde{\ell}^{\pm} \to \ell^{\pm}\chi_1^0$) = 1. For smuons and staus, these limits are independent of the MSSM parameters. For selectrons, complementary analyses

Table 7
Lower limits at 95% C.L. on the slepton masses for $\Delta M > 15$ GeV/c^2, with the hypothesis BR($\tilde{\ell}^{\pm} \to \ell^{\pm}\chi_1^0$) = 1. For staus, the bound corresponding to the minimum cross section (as explained in the text) is also given. In the case of selectrons, the limits are given for $\mu = -200$ GeV/c^2 and $\tan\beta = 2$

Channel	$m(\tilde{\ell}) >$ obtained	$m(\tilde{\ell}) >$ expected
$\tilde{e}_R$	95 GeV/c^2	96 GeV/c^2
$\tilde{\mu}_R$	88 GeV/c^2	87 GeV/c^2
$\tilde{\tau}_R$	79 GeV/c^2	83 GeV/c^2
$\tilde{\tau}$(min)	76 GeV/c^2	81 GeV/c^2

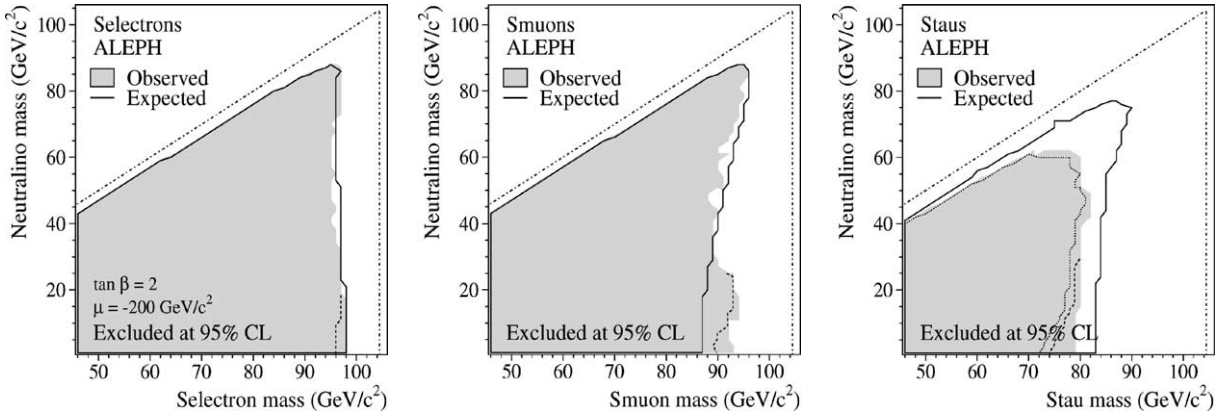

Fig. 4. Excluded regions at 95% C.L. in the $m_{\tilde{\ell}_R}$ versus $m_{\chi_1^0}$ plane from slepton searches. The observed (shaded area) and expected (solid curve) limits are given for BR($\tilde{\ell}^{\pm} \to \ell^{\pm}\chi_1^0$) = 1. For selectrons, $\mu = -200$ GeV/c^2 and $\tan\beta = 2$ are assumed. The dashed curves give the observed limits when slepton cascade decays are taken into account. For staus, the dotted curve gives the most conservative limit, obtained for $\theta_{\tilde{\tau}} \simeq 52°$ and with cascade decay taken into account. For the dashed and dotted curves, BR($\tilde{\ell}^{\pm} \to \ell^{\pm}\chi_1^0$) is computed with the values $\mu = -200$ GeV/c^2 and $\tan\beta = 2$, and a zero efficiency for the selection of the topologies arising from cascade decay is assumed. The kinematically accessible region at 209 GeV is indicated by the vertical dash-dotted lines. The diagonal dash-dotted lines show the boundary of the domain allowed in the MSSM for a neutralino LSP.

and a scan on the relevant MSSM parameters allow an absolute mass lower limit to be extracted. The result of such a study is presented in Ref. [22].

7. Conclusions

Searches for scalar lepton pair production have been performed in the data sample collected by the ALEPH experiment at LEP2 at centre-of-mass energies up to 209 GeV. The numbers of candidate events observed are consistent with the background expected from Standard Model processes.

In the framework of the MSSM, 95% C.L. mass exclusion regions have been obtained for selectrons, smuons and staus in the plane $(m_{\tilde{\ell}}, m_{\chi_1^0})$. In particular, mass lower limits for smuons and staus are set at 88 and 76 GeV/c^2, respectively, for a mass difference between the slepton and the lightest neutralino in excess of 15 GeV/c^2 and for a slepton decay branching ratio into $\ell\chi_1^0$ of 100%. These limits are independent of the MSSM parameters. Under the same assumptions, and with $\mu = -200$ GeV/c^2 and $\tan\beta = 2$, a lower limit of 95 GeV/c^2 is set on the selectron mass.

Acknowledgements

It is a pleasure to congratulate our colleagues from the accelerator divisions for the outstanding operation of LEP2, especially in its last year of running during which the accelerator performance was pushed beyond expectation. We are indebted to the engineers and technicians in all our institutions for their contributions to the excellent performance of ALEPH. Those of us from non-member states wish to thank CERN for its hospitality and support.

References

[1] H.P. Nilles, Phys. Rep. 110 (1984) 1;
H.E. Haber, G.L. Kane, Phys. Rep. 117 (1985) 75;
D.E. Groom et al., Eur. Phys. J. C 15 (2000) 1.
[2] ALEPH Collaboration, Phys. Lett. B 407 (1997) 377;
ALEPH Collaboration, Phys. Lett. B 433 (1998) 176.
[3] ALEPH Collaboration, Phys. Lett. B 469 (1999) 303.
[4] ALEPH Collaboration, Phys. Lett. B 499 (2001) 67.
[5] DELPHI Collaboration, Phys. Lett. B 489 (2000) 38;
L3 Collaboration, Phys. Lett. B 471 (1999) 280;
OPAL Collaboration, Eur. Phys. J. C 14 (2000) 51.
[6] ALEPH Collaboration, Nucl. Instrum. Methods A 294 (1990) 121.
[7] ALEPH Collaboration, Nucl. Instrum. Methods A 360 (1995) 481.
[8] Yu.L. Dokshitzer, J. Phys. G 17 (1991) 1441.
[9] S. Katsanevas, P. Morawitz, Comput. Phys. Commun. 112 (1998) 227.
[10] E. Barberio, Z. Wąs, Comput. Phys. Commun. 79 (1994) 291.
[11] S. Jadach, Z. Wąs, R. Decker, J.H. Kühn, Comput. Phys. Commun. 76 (1993) 361.
[12] S. Jadach, W. Placzek, B.F.L. Ward, Phys. Lett. B 390 (1997) 298.
[13] S. Jadach, Z. Wąs, Comput. Phys. Commun. 36 (1985) 191.
[14] J.A.M. Vermaseren, in: G. Cochard, P. Kessler (Eds.), Proceedings of the IVth International Workshop on Gamma Gamma interactions, Springer-Verlag, 1980.
[15] M. Skrzypek, S. Jadach, W. Placzek, Z. Wąs, Comput. Phys. Commun. 94 (1996) 216.
[16] T. Sjöstrand, Comput. Phys. Commun. 82 (1994) 74.
[17] GEANT detector description and simulation tool, CERN Program Library, CERN-W5013 (1993).
[18] J.F. Grivaz, F. Le Diberder, Complementary analysis and acceptance optimization in new particle searches, LAL preprint #92-37 (1992);
ALEPH Collaboration, Phys. Lett. B 384 (1996) 427.
[19] R.A. Fisher, Ann. of Eugenics 7 (1936) 179.
[20] A.L. Read, Modified frequentist analysis of search results (The CLs Method), CERN-OPEN-2000-205, 81.
[21] R.D. Cousins, V.L. Highland, Nucl. Instrum. Methods A 320 (1992) 331.
[22] ALEPH Collaboration, Lower mass limit for the MSSM selectron and sneutrino obtained with the ALEPH detector, contribution #236 to the IECHEP, Budapest, Hungary, 12–18 July, 2001, ALEPH-CONF 2001-047, http://alephwww.cern.ch/ALPUB/oldconf/summer01/33/sel_limit.ps.